

**mechanical design of DNA nanostructures**

Journal:	<i>Nanoscale</i>
Manuscript ID:	NR-REV-12-2014-007153.R1
Article Type:	Feature Article
Date Submitted by the Author:	22-Jan-2015
Complete List of Authors:	Castro, Carlos; The Ohio State University, Mechanical and Aerospace Engineering; The Ohio State University, Biophysics Graduate Program Su, Haijun; The Ohio State University, Mechanical and Aerospace Engineering Marras, Alexander; The Ohio State University, Mechanical and Aerospace Engineering Zhou, Lifeng; The Ohio State University, Mechanical and Aerospace Engineering Johnson, Joshua; The Ohio State University, Biophysics Graduate Program

Mechanical Design of DNA nanostructures

Carlos E. Castro^{1,2,*}, Hai-Jun Su¹, Alexander E. Marras¹, Lifeng Zhou¹, Joshua Johnson²

¹Department of Mechanical and Aerospace Engineering, The Ohio State University, Columbus,
OH 43210

²Biophysics Graduate Program, The Ohio State University, Columbus, OH 43210

*to whom correspondence should be addressed

Abstract:

Structural DNA nanotechnology is a rapidly emerging field that has demonstrated great potential for applications such as single molecule sensing, drug delivery, and templating molecular components. As the applications of DNA nanotechnology expand, a consideration of their mechanical behavior is becoming essential to understand how these structures will respond to physical interactions. This review considers three major avenues of recent progress in this area: 1) measuring and designing mechanical properties of DNA nanostructures, 2) designing complex nanostructures based on imposed mechanical stresses, and 3) designing and controlling structurally dynamic nanostructures. This work has laid the foundation for mechanically active nanomachines that can generate, transmit, and respond to physical cues in molecular systems.

Introduction:

Biological cells rely on biomolecular machinery to perform essential processes such as physical and chemical communication with their environment. The function of these macromolecules, including proteins, DNA, and RNA, is dependent on specific characteristics, namely geometry, chemical functionality, and mechanical behavior, which are encoded in primary amino acid or nucleotide sequences. Molecular motors, for example, follow tracks with precisely spaced and oriented docking sites, hydrolyze ATP, and generate mechanical forces to transport intracellular cargo or drive cellular motion. Biomolecular nanotechnology has made great strides in developing the capacity to mimic these functional characteristics (geometry, chemical functionality, and mechanical behavior) in designed systems fabricated via molecular self-assembly. Amino acid based design^{1, 2} affords the long-term possibility of reaching the functional scope of cellular proteins such as molecular motors or enzymes; however, the complexity of interactions that govern amino acid folding and enable chemical functionality make de novo design of precise protein geometries highly challenging. DNA assembly, on the other hand, is governed by well-understood Watson-Crick base-pairing interactions³. While the chemical functionality of DNA is limited relative to proteins, the programmable nature of base-pairing assembly has provided a foundation for the rapidly progressing field of structural DNA nanotechnology.

Since its inception in the early 1980's through the foundational work of Nadrian Seeman⁴, structural DNA nanotechnology has evolved as a field of geometric design starting with lattices (geometrically connected immobile DNA junctions⁴⁻⁶), then leading to DNA nanotubes and arrays⁷⁻¹¹, and more recently developing shapes of almost arbitrary geometric complexity with the development of scaffolded DNA origami¹² and its extension to 3D¹³.

The majority of current applications for DNA origami rely primarily on the ability to design complex and mechanically stiff nanoscale geometries. Examples include nanotubes to assist structure alignment for solution NMR studies¹⁴, nanopores for single molecule sensing¹⁵⁻¹⁷, platforms for super-resolution fluorescence microscopy¹⁸⁻²⁰, templates for nanotubes²¹, nanoparticles²²⁻²⁵, and vehicles for small molecule drug delivery²⁶⁻²⁸. Other efforts have exploited the ability to modify DNA in order to expand the range of chemical functionality by

integrating small molecules^{29, 30}, DNA aptamers³¹⁻³³, peptides³⁴, proteins^{32, 35, 36}, or other biomolecules^{16, 37, 38}. Recent examples demonstrating the power of these chemical modifications include coupling DNA origami nanostructures with motor proteins for studies of motor cooperativity³⁹ and integration of DNA origami nanostructures into lipid membranes via carbohydrate modifications^{16, 38} thus opening possibilities to study cell membrane surfaces and interactions.

While the chemical functionality of DNA nanostructures has been expanded through modification, the mechanical functionality beyond designing specific geometries has been less widely explored. DNA origami nanostructures, in particular, are often designed with a specific number of helices in order to approximate some complex geometry, but with relatively little consideration for the resulting mechanical behavior. Generally, this approach results in sufficient stiffness to minimize thermal fluctuations and maintain a well-defined shape that defines the function of the nanostructure. However, just as incorporating chemical modifications enhances functional scope, specific consideration and design of mechanical behavior can open possibilities to a broad range of new applications that include physical communication with the local environment. Here we highlight recent progress in area of DNA origami nanotechnology specifically with regards to 1) designing and characterizing mechanical stiffness, 2) exploiting mechanical stress in DNA nanostructure design, and 3) designing and actuating dynamic behavior (i.e. motion and reconfiguration) of DNA nanostructures.

Designing and characterizing mechanical stiffness of DNA origami nanostructures

The mechanical properties of double-stranded DNA (dsDNA) have been widely-studied⁴⁰⁻⁴³ since they play a critical role in gene regulation and DNA replication and repair. Compared to structural biopolymers (e.g. actin or microtubules), DNA is flexible, which allows it to be tightly packaged into the nucleus and undergo structural dynamics critical for DNA processing. Structural DNA nanotechnology connects several dsDNA helices into a compact geometry to create objects that can be several orders of magnitude stiffer than the constituent DNA. Ultimately, the stiffness of designed DNA nanostructures are a result of the physical properties

of DNA, the number, locations, and stiffness of connections points, and the geometry of the structure.

While the mechanics of DNA are well characterized, the stiffness of DNA junctions has primarily been investigated in terms of physiologically relevant Holliday junctions^{44, 45}, although recent computational efforts have begun to consider junction stiffness in DNA nanostructures⁴⁶⁻⁴⁹. Here we outline recent progress made in quantifying and designing the mechanical behavior of designed DNA nanostructures. We focus our discussion on the persistence length (L_P), defined as $L_P = K_B/k_bT$ (K_B is the bending stiffness, k_b is Boltzmann's constant, and T is absolute temperature) since mechanical characterization has largely focused on quantifying L_P .

Direct measurement of the stiffness of designed DNA nanostructures started with the development of DNA nanotubes (circumferentially connected helices) several μm in length^{7, 9, 10}. Rothmund et al.⁹ first measured the average persistence length (L_P) of DNA nanotubes 7-20 nm in diameter as, $L_P = 3.9 \mu\text{m}$, approximately two orders of magnitude larger than dsDNA ($L_{P,dsDNA} = 50\text{nm}$ ^{40, 43}). Yin and co-workers⁵⁰ later developed an approach to control the diameter of DNA nanotubes by specifying the number of helices in the cross-section. Schiffels et al.⁵¹ found L_P of these nanotubes ranged from 2.0 μm for a 5-helix tube up to 16.8 μm for a 10-helix tube (**Figure 1a, black circles**), closely following the behavior of rigidly coupled helices. Persistence length measurements of scaffolded DNA origami nanostructures have been limited to small cross-sections that form objects $>100\text{nm}$ in length. Liedl and co-workers first measured L_P of gel-purified 6-helix bundles (hb) as 1.6 μm ⁵², and Kauert et al.⁴⁶ used magnetic tweezers to measure L_P for 4-hb and 6-hb of 0.74 μm and 1.88 μm , respectively. Here, we present a conformational distribution for similar 6-hb (**Figure 1b**), which was used to determine $L_P = 1.4 \mu\text{m}$ by measuring the splay width of the conformational distribution as a function of arc length⁵³ (details in Supplemental).

Figure 1a shows a summary of persistence length measurements for DNA nanotubes and scaffolded DNA origami bundles, and for comparison the persistence length scaling of actin bundles⁵⁴ as a function of the number of polymers (i.e. dsDNA helices or actin filaments) in the bundle, N . The gray shaded region shows the limits of loosely coupled ($L_P \sim N$) and rigidly coupled DNA origami nanostructures, which can exceed the typical $L_P \sim N^2$ scaling for rigidly

coupled bundles⁵⁴ because they are not close packed (i.e. the cross-section contains voids). Direct calculation of the rigidly coupled limit (i.e. infinite stiffness of cross-overs prevents any relative motion of connected helices) for the four cross-sections shown (details in Supplemental) reveals an upper limit scaling behavior of $L_P \sim N^{2.42}$ (note that this scaling behavior would vary with different cross-sectional geometries). A simple power law fit to the measured persistence length values for scaffolded DNA origami nanostructures reveals a scaling of $L_P \sim N^{1.94}$, suggesting DNA origami cross-over connections result in stiff, but not rigid coupling between helices. In other words, some shearing between helices in the bundle may occur, but cross-over connections provide significant resistance to that shearing.

Using this scaling, we can estimate the bending stiffness of larger DNA origami honeycomb cross-sections, for example the 18-hb or 54-hb shown as insets in **Figure 1a**. This approach provides only rough estimates for L_P of larger cross-sections. Previous work has shown that the L_P of polymer bundles only follows simple power law scaling in the rigidly coupled or loosely coupled limits, and a more detailed theoretical⁵⁴ or computational approach^{47, 48} would be required to accurately predict the stiffness of larger cross-sections. However, these simple estimates at least indicate that nanostructures as stiff as actin filaments ($L_P = 18 \mu\text{m}^{55}$) and potentially even microtubulues ($L_P = 100\text{-}5000 \mu\text{m}^{55, 56}$) could be made using scaffolded DNA origami.

To illustrate the thermal fluctuations of DNA origami nanostructures, we performed stochastic simulations of DNA nanostructure configurations. Briefly, bundle trajectories were reconstructed as chains of segments where the change in angle between segments, $\Delta \theta$, was defined according to the tangent angle correlation equation, $\langle \cos(\Delta\theta) \rangle = \exp(-\Delta s/2L_P)$. The factor of 2 is present to reproduce 2D conformational distributions. The results for conformational distributions were not sensitive to selection of the segment length provided $L_{segment}/L_{bundle} \lesssim 0.01$. Details of simulations are provided in Supplemental Information. **Figure 1c** shows simulations of conformational distributions using persistence lengths obtained from the scaling behavior in **Figure 1a** for 6-hb, 18-hb, and 54-hb. Here we assumed the total number of base-pairs was limited to a typical DNA origami scaffold (7560 bp)^{13, 57}, hence structures with larger cross-sections are shorter in length. The 6-hb simulation closely matches the experimental data. These simulations illustrate that DNA origami nanostructures containing 18-hb or more helices in the

cross-section are not subject to significant thermal fluctuations, and hence maintain a well-defined shape.

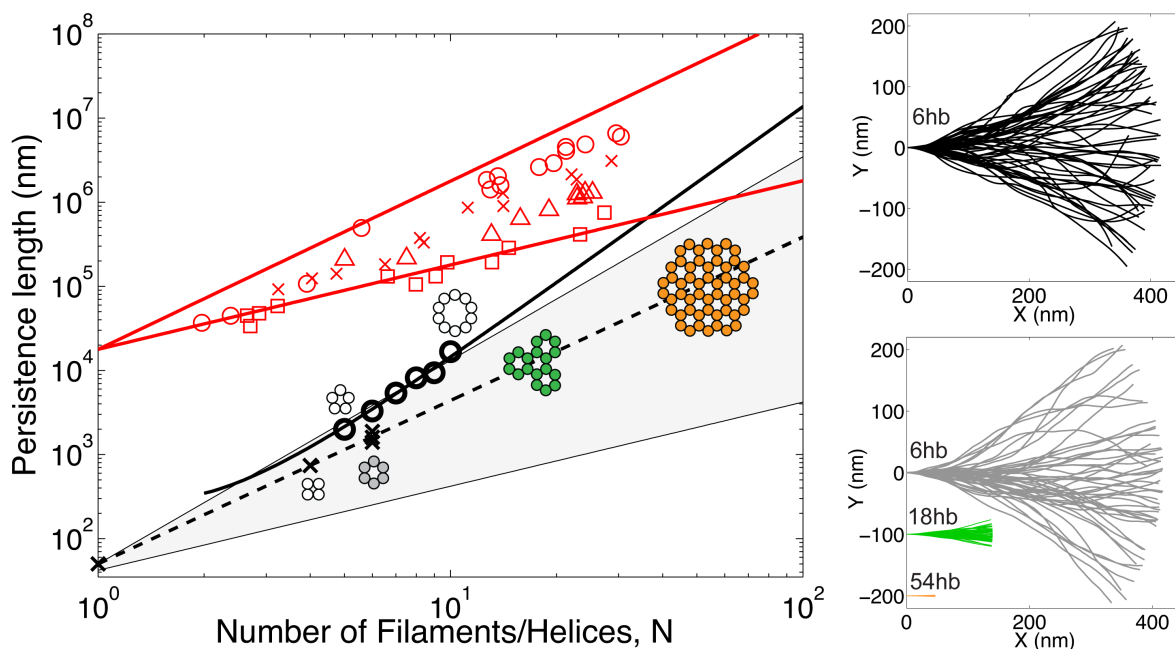


Figure 1: Mechanical Properties of DNA origami nanostructures. (a) Bundling dsDNA helices into compact cross-sections increases persistence length, L_P , similar to bundling of actin filaments. The red data shows persistence length measurements of actin bundles with different concentrations of bundling protein (different shapes) and the corresponding limits of uncoupled (L_P scales with N) and rigidly coupled (L_P scales with N^2) filaments (data reprinted from⁵⁴ with permission from Nature Publishing Group and Dr. Andreas Bausch). The shaded gray region shows similar limits for uncoupled and rigidly coupled DNA helices. DNA nanotubes^{50, 51} (black circles) closely follow the rigidly coupled limit and can even exceed the N^2 scaling due to swelling of the cross-section. Schiffels et al.⁵¹ developed a model to predict L_P assuming rigid coupling and accounting for swelling (solid black line). L_P of scaffolded DNA origami nanostructures with 4-helix⁴⁶ and 6-helix^{46, 52} cross-sections approximately follow a power law scaling behavior of $N^{1.94}$ (dashed black line). Schematics of cross-sections are shown next to the corresponding data. The green and orange cross-sections are potential cross-sections that could have stiffness in the range of actin filaments. (b) We measured shape distributions of DNA origami 6-hb revealing $L_P = 1.4 \mu\text{m}$, in good agreement with other measurements. (c) Stochastic

simulations of shape distributions closely match 6-helix bundle (hb) experiments, and demonstrate the reduced shape fluctuations for larger cross-sections.

A few studies have explored the mechanical behavior and design of mechanical properties of DNA origami nanostructures more extensively than by just considering the bending persistence length. For example, Kauert et al.⁴⁶ measured the torsional persistence length of 4-helix and 6-helix bundles to be 390 nm and 530 nm, respectively; Plesa and co-workers⁵⁸ demonstrated that the bending stiffness of DNA origami nanoplates was critical to their functional ion conductance; and Pfitzner et al.⁵⁹ exploited the stiffness of DNA origami beams to improve the resolution of force spectroscopy experiments. In addition, our collaborative team⁶⁰ has recently explored the design of deformable (compliant) DNA nanostructures with tunable stiffness. Going forward, consideration of mechanical properties will be a critical factor in the design of devices that must withstand and transmit forces through interactions with other materials and molecules. The development and use of computational tools, such as CANDO^{47,57} or recent efforts in molecular dynamics⁴⁸ and lattice-free structure prediction⁴⁹, will undoubtedly provide useful tools for predicting and interpreting mechanical behavior of DNA nanostructures.

Exploiting mechanical stress in DNA nanostructure design

In biological cells, DNA is bent and twisted in order to be packaged into chromatin resulting in mechanical strain energy stored in the deformed polymer. This stored mechanical energy results in local stresses, often referred to as residual stress in macroscopic systems, that plays a critical role in the unwrapping required for DNA processing. These residual stresses can be programmed into DNA origami nanostructures to induce additional geometric complexities in design, such as curvature or twist, much like a tensed string results in bending of a bow in a bow and arrow. This is achieved by introducing local tensile, compressive, or torsional stresses that combine to induce deformation of the overall structure. **Figure 2** shows several examples of complex DNA nanostructures where the geometry relies on residual stresses in the constituent DNA helices.

While prior efforts had exploited mechanical properties, such as flexibility, in DNA assembly⁶¹, the use of stored mechanical energy to design deformed structures was first demonstrated by Dietz and co-workers⁶² who locally deleted or added base-pairs between DNA origami cross-over connections to introduce stresses that caused bending or twist of the overall structure

(**Figure 2a**). The degree of bending or twist could be programmed according to the amount of stress (i.e. number of base-pairs added or deleted) and the overall bending or torsional stiffness of the structure. Han and co-workers⁶³ later established control of curvature in two directions by forcing cross-over connections between helices of different lengths to induce bending in the direction of the shorter helices. By spatially arranging longer and shorter helices in parallel, they created fully closed spherical objects (**Figure 2b**). Han et al.⁶⁴ also developed a similar design framework by connecting helices in a cross-hatched pattern where perpendicular branched connections could be made between parallel helices of different lengths to induce 1D or 2D curvature (**Figure 2c**).

The previously described approaches rely on local stresses to create structures with complex curvature or twist that are still mechanically stiff and structurally well-defined (i.e. undergo minimal thermal fluctuations). To access a broader range of mechanical behavior, Liedl et al.⁵² exploited the entropic elasticity of single-stranded DNA (ssDNA) to develop DNA origami tensegrity structures (**Figure 2d**). In their DNA origami tensegrity structures, tension in ssDNA components is balanced with compression or bending of dsDNA components. The overall stiffness of the structures depends on both dsDNA and ssDNA components, thereby affording access to a large range of stiffness. Liedl and co-workers further developed a method to tune the length of ssDNA components by partially folding them into small DNA origami bundles as depicted in **Figure 2d** (right). We have recently expanded on this method to create DNA origami compliant (deformable) nanostructures with tunable geometry and stiffness⁶⁰. Our approach exploits entropic elasticity of ssDNA to bend an anisotropic stiff dsDNA component, a single layer of 6-helices. Examples are shown in **Figure 2E**. Both the stiffness and geometry of the structure can be precisely controlled by modifying the length of the ssDNA connections, which we achieved by shifting ssDNA between the tension-bearing connections and a neighboring ssDNA loop. These two efforts demonstrate the potential to enhance DNA origami design, in particular mechanical functionality, through the incorporation of ssDNA.

In all of these approaches, the cumulative base-pairing energy outweighs the local mechanical strain energy due to deformation of dsDNA so that the structure is still stable, although Dietz et al.⁶² noted that structures with higher mechanical strain tended to fold with lower yield. Ultimately, the magnitude of mechanical stress that can be introduced or the localized force that

can be applied is limited by the base pairing energy of the structure. However, design modifications (e.g. arranging helices in a shear as opposed to unzipping conformation⁶⁵), locally integrating more stable components (e.g. peptide nucleic acids⁶⁶), or even chemical modifications (e.g. local covalent cross-links between strands⁶⁷) could allow for mechanically enhanced structures that can withstand and transmit larger forces or store more mechanical energy. Furthermore, methods could be developed in the future to release this energy to mimic force generation of molecular motors⁶⁸ or biological springs⁶⁹.

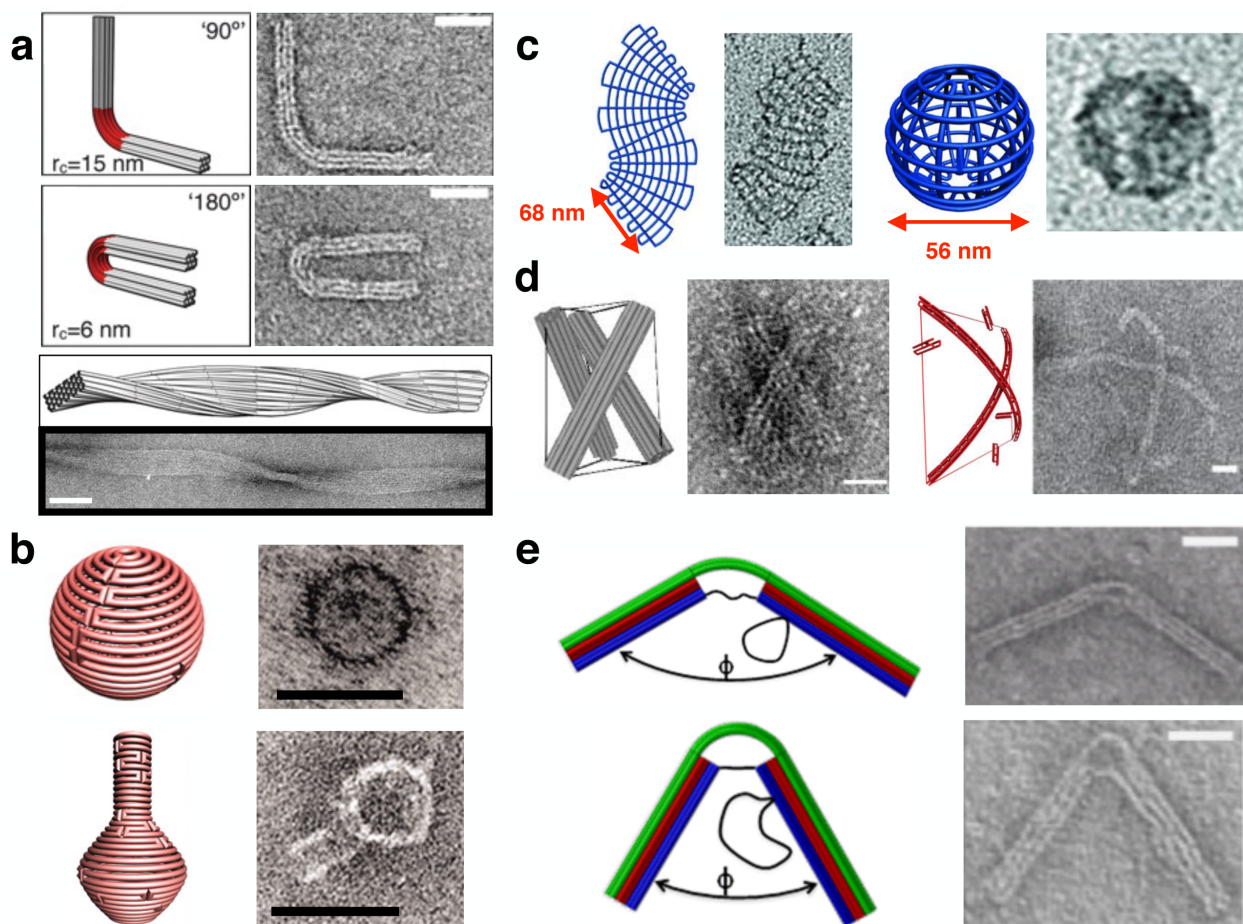


Figure 2: Exploiting mechanical stress in DNA nanostructure design. (a) Curvature or twist can be programmed by adding or deleting base pairs between cross-over connections in DNA origami structures to introduce local stresses⁶². Scale bars are 20nm (top) and 50nm (bottom). (b) Similarly, forcing connections between mismatched lengths of dsDNA with helices arranged in parallel⁶³ or (c) perpendicularly in a cross-hatched pattern⁶⁴ enables programming curvature and making curved shell or spherical objects. (d) The use of ssDNA allows application of entropic

forces that can induce compression (left) or bending (right) of dsDNA components⁵². (e) Bending can be directed using anisotropic dsDNA components to make components with tunable curvature⁶⁰. In addition tuning lengths of ssDNA by partially folding it into dsDNA, as in (d) on the right, or by shifting ssDNA length between to a “reservoir” loop, as in (e), allows tuning the tension in the ssDNA. Combining ssDNA and dsDNA ultimately allows access to a broader range of mechanical behavior. Scale bars are 50nm in (b) and 20nm in (d,e).

Designing and actuating dynamic behavior of DNA nanostructures

Dynamic behavior including thermal fluctuation, conformational changes, and directed motion, is a key aspect of the function of biomolecular machinery. The ability to design this dynamic behavior in synthetic systems is a central challenge of biomolecular nanotechnology. Although the majority of current applications of DNA nanostructures rely primarily on well-defined geometric design, some significant advances have been made since the early stages of the field in fabricating and controlling dynamic behavior of DNA nanostructures. These dynamic structures have been designed to achieve complex conformational changes (**Figure 3a,b**^{70, 71}), detect molecular binding events (**Figure 3c,d**^{72, 73}), or encapsulate and then release compounds or molecules (**Figure e-h**^{31, 32, 74, 75}).

The first controllable designed DNA nanostructure, introduced by Mao and co-workers⁷⁶, exploited the B-Z transition of DNA, triggered by changing solution conditions, to make switchable devices made from a few strands of DNA. Since their breakthrough, research efforts to fabricate dynamic DNA nanosystems have primarily focused on nanostructures where conformational changes can be triggered by molecular binding events, or by strand invasion (i.e. strand displacement)⁷⁷, whereby a DNA strand in the folded structure is exchanged with a DNA input strand from solution usually mediated by initial binding to a ssDNA overhang (i.e. toehold)⁷⁸. The strand invasion approaches started with Yurke et al.⁷¹ who fabricated DNA “tweezers” comprising three strands that could be opened or closed with DNA inputs, shown schematically in **Figure 3a**. Yan and co-workers extended this approach to demonstrate controlled rotational motion in a DNA nanostructure array⁷⁹. These works laid a foundation for several reconfigurable structures with conformational changes triggered by binding of DNA

inputs⁷⁹⁻⁸³. These systems achieve small (~1-10nm) motions that in some cases could be accumulated on a track to add up to ~100 nm⁸⁴ and transport⁸⁵ or even assemble⁸⁶ nanoscale components. Similar strand displacement approaches form the basis of DNA-based molecular computing.^{87, 88}

The establishment of DNA origami techniques provided a platform to direct local strand reconfiguration, for example to guide DNA walkers⁸⁴, harness logic steps⁸⁹, control molecular binding⁷³, or locally reconfigure strands on a DNA platform⁹⁰. Building on these approaches, strand displacement has been used to control larger-scale structural transitions in DNA origami systems. For example, Han et al.⁷⁰ created a DNA origami Möbius strip (one-sided ribbon structure) that could be cut open via strand displacement reactions to approximately double in size, depicted schematically in **Figure 3b**. Other recent efforts have expanded this work to achieve reversible actuation of DNA nanostructures. Kuzuya et al.⁷³ demonstrated reversible actuation in a DNA origami tweezer-like structure that could be actuated into a closed state upon binding of biomolecules (e.g. streptavidin or oligonucleotides) and then re-opened by DNA strand displacement (**Figure 3d**). Recently, Kuzyk and co-workers⁹¹ used a similar scissor-like device to actuate changes in chirality of gold nanorods enabling reversible control of plasmonic interactions. Feng and co-workers⁹² demonstrated that reversible conformational changes could be executed in a lattice system where repeat units in the lattice were extended and subsequently shortened, both via DNA strand invasion. Both Feng and Kuzuya implemented distributed actuation methods where DNA inputs bind to or displace multiple strands on the structure to drive conformational changes.

The strand invasion concept has also been implemented to construct DNA containers for drug release^{31, 32, 74, 75} (**Figure 3e-h**). These approaches exploit the energy of DNA base-pairing that is achieved during the initial self-assembly process to hold the structure in a “closed” configuration while molecules are trapped inside. When local connections are released by strand displacement, the system relaxes to an “open” or unconstrained state where molecules diffuse out of the container or at least are exposed to solution. Douglas et al.³² (**Figure 3g**) and Banerjee et al.³¹ (**Figure 3h**) expanded the scope of the strand invasion process using DNA aptamers to lock containers closed that could then open in the presence of a non-nucleotide target molecules (i.e.

proteins or small molecules). This use of DNA aptamers provides access to a diverse range of interaction targets in vitro or in vivo.

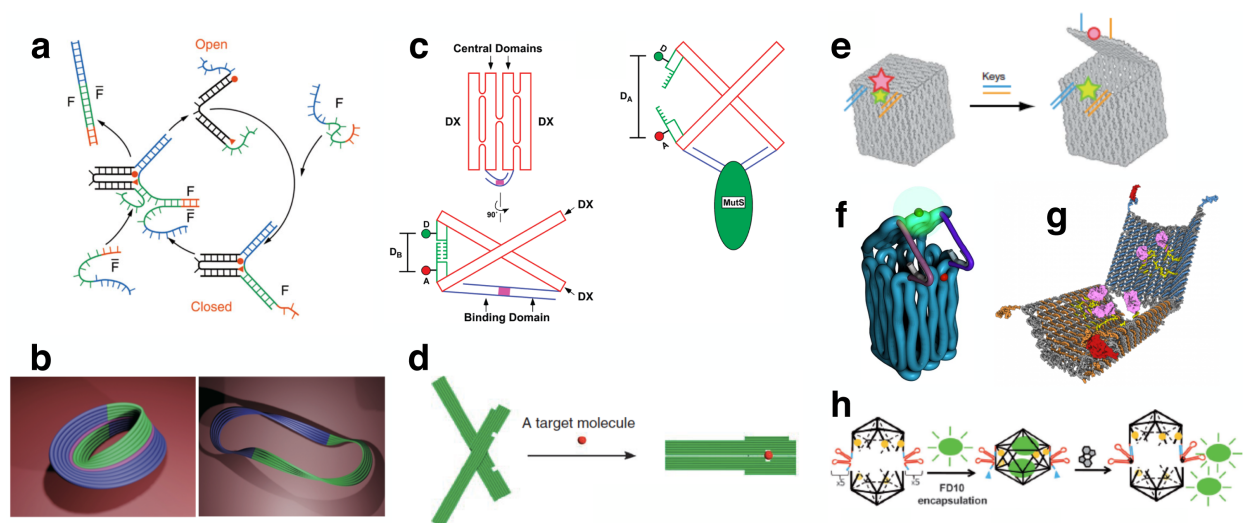


Figure 3: Examples of mechanically dynamic nanostructures. Examples of dynamic DNA nanostructures include: 1) (a,b) structures designed to demonstrate complex conformational changes^{70, 71}, 2) (c,d) devices that detect molecular binding events^{72, 73}, or 3) (e-h) containers intended to encapsulate and subsequently release cargo^{31, 32, 74, 75}.

Our research team has recently expanded on dynamic DNA-based design by adopting an engineering machine design approach⁹³. Like in macroscopic machine design, our approach starts with fabricating joints with constrained motion in specified rotational or linear degrees of freedom. Our general approach for designing constrained motion is to combine precisely designed stiff dsDNA components with selectively placed ssDNA strands so that the geometry of the stiff components and the placement of the flexible connections allow motion only in specific degrees of freedom. We call these nanostructures DNA origami mechanisms (DOM). **Figure 4a** and **4b** show schematics and TEM images of DNA origami joints with a single dominant angular (**Figure 4a**) or linear (**Figure 4b**) degree of freedom. While angular motion has been previously demonstrated in several of the aforementioned studies, our work⁹³ was the first to demonstrate controlled linear motion.

In our framework, more complex motion can be designed by incorporating multiple joints into a single structure. These joints can move independently as in the case of the universal joint

presented here (**Figure 4c**), which has two angular degrees of freedom (gel analysis and additional TEM images are provided in the Supplemental information); or they can be integrated into a mechanism, such as the crank-slider⁹³ (**Figure 4d**), which comprises components with rotational and linear motion that are coupled resulting in a mechanism with 2D motion with a single degree of freedom. This machine-like design approach opens the door for designing complex devices with well-defined motion and/or force transmission. For example, the crank-slider could translate a binding event that drives rotational motion (previously demonstrated by others^{72, 73, 94}) into linear motion to generate a linear force or facilitate a downstream interaction. Alternatively, it could generate a torque in response to a linear displacement.

A major direction in the field of biomolecular nanotechnology is to reproduce the complex function of natural molecular machinery. In contrast, a major cornerstone of our efforts in DNA origami nanotechnology relies on drawing parallels to and implementing ideas from macroscopic engineering structure and machine design. The ability to design stiff components of essentially arbitrary geometric complexity and integrate constrained motion in specified degrees of freedom enables a modular approach to piece components together in machines that resemble macroscopic systems. To illustrate this concept, we have fabricated a DNA origami scissor mechanism (**Figure 4e**) that resembles and functions similarly to a macroscopic scissor lift. The DNA origami scissor mechanism is constructed by first decomposing the mechanism into a unit cell that has three rotational degrees of freedom (**Figure 4e** left). This unit was polymerized by sticky end interactions to form a 1D array where the rotational degrees of freedom couple to achieve linear motion. The TEM images on the right of **Figure 4e** depict an open and an extended state of a 3-mer polymerized scissor mechanism. In this case, this motion was achieved simply by thermal fluctuation along the constrained motion path. Our future work will pursue actuation of this scissor mechanism and other extendable DNA origami mechanisms to couple distributed molecular actuation to force generation and $\sim\mu\text{m}$ scale motion. Full design details, folding protocols, gel analysis, and additional TEM images for the scissor mechanism are available in the Supplemental information.

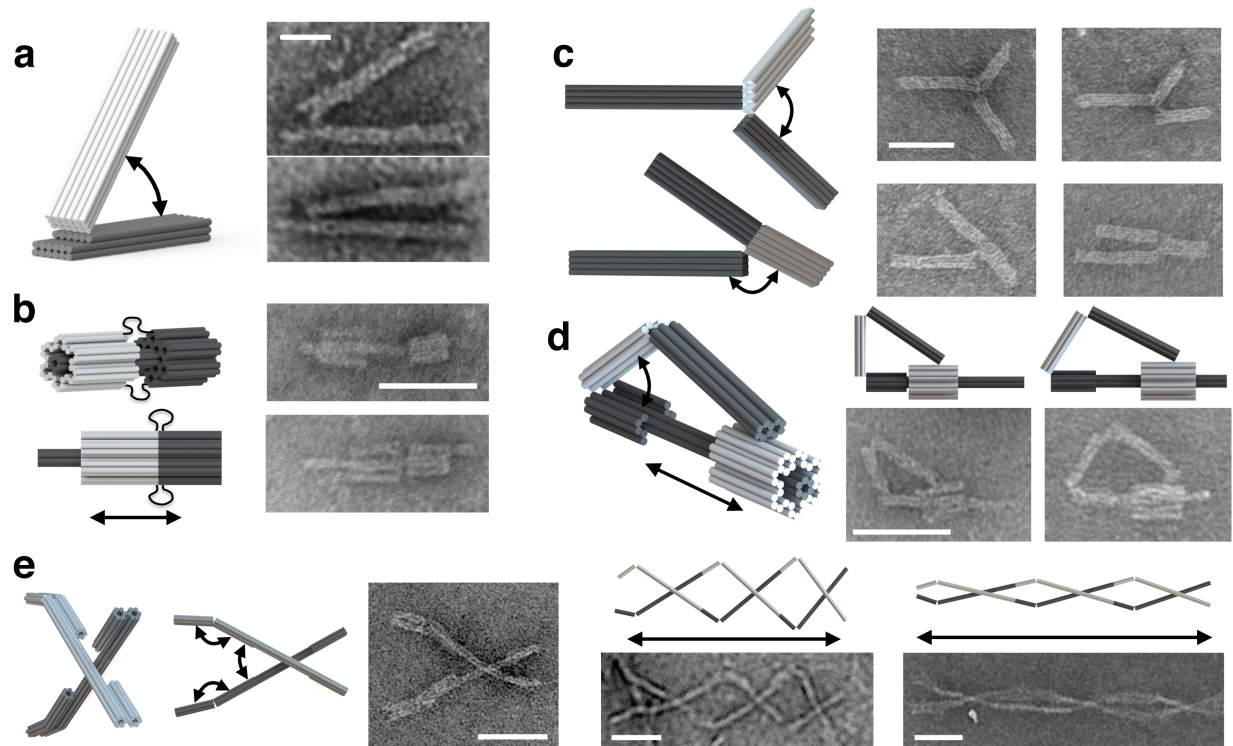


Figure 4: DNA origami machine components. A framework for designing DNA origami mechanisms and machines⁹³ starts with designing basic joints with motion in specified degrees of freedom. Schematics and TEM images depict joints with (a) a single dominant rotational or (b) linear degree of freedom. (c) DNA origami joints can also exhibit multiple independent degrees of freedom as in the universal joint, or (d) these joints can be integrated into a mechanism which couples rotational to linear motion, as in the slider-crank. These mechanisms can be assembled into larger structures that resemble macroscopic machines as demonstrated by the scissor mechanism in (e). The DNA origami scissor mechanism was constructed by first assembling the structural unit (left) and then polymerizing a 1D array (right) that couples rotational motion of the unit into linear motion of the mechanism. The scale bar in (a) is 20nm and all other scale bars are 50nm. The structures in (a), (b), and (d) are reprinted from our previous work⁹³ with permission from PNAS. The structures in (c) and (e) are presented here for the first time. Scale bars are 20 nm in (a) and 50 nm (b-e).

Concluding remarks:

Here we have detailed major strides in designing and exploiting the mechanical behavior of DNA origami nanostructures, specifically in characterizing and designing mechanical stiffness, exploiting mechanical stress in geometric design, and fabricating and actuating dynamic DNA nanostructures. In particular, the recent progress in DNA origami mechanism (DOM) design paves the way to mimic the macroscopic machines for designing dynamic nanostructures with controllable complex motion. In the future, expanding the range of accessible mechanical behavior of DNA origami nanostructures will greatly expand the scope of potential applications. Already some current applications exploit the mechanical behavior of DNA nanostructures, for example to obtain improved resolution in force spectroscopy⁵⁹, detect DNA-protein binding interactions⁷², or exploit flexibility of ssDNA to facilitate enzyme activity⁹⁵.

Further advances in understanding and modeling the mechanical behavior of designed DNA nanostructures will enable improved design of mechanical properties, dynamic behavior, and force generation mechanisms similar to natural molecular machines. A promising future direction for mechanical design of DNA nanostructures is the direct design of complex DNA origami energy landscapes that include multiple stable states and energy barriers to regulate conformational dynamics and physical interactions with the local environment. In the future, designed mechanical behavior can be integrated with precise geometry and chemical functionality to create DNA-based nanomachines that can transmit and generate forces, and more generally perform chemical and mechanical work, to achieve complex functions such as the ability to sense and respond to their environment; manipulate, assemble, and transport molecular components; actuate and control chemical reactions; and even store and convert energy. A particularly exciting possibility would be interfacing these nanomachines with DNA-based molecular computing to achieve dynamic mechanical systems that can process and generate information. With the ability to design and control complex mechanical behavior, combined with chemically functionalizing DNA nanostructures and recent advances towards fabricating larger DNA origami systems⁹⁶ it seems the functional scope of DNA nanotechnology will continue to expand for years to come.

Acknowledgements:

This work was supported primarily by the National Science Foundation under Grant No: CMMI-1235060 and Grant No: CMMI-1228104. Any opinions, finding, conclusions or recommendations expressed in this material are those of the authors and do not necessarily reflect the views of the funding agency.

REFERENCES

1. D. Baker, *Philosophical transactions of the Royal Society of London. Series B, Biological sciences*, 2006, 361, 459-463.
2. T. Aida, E. W. Meijer and S. I. Stupp, *Science*, 2012, 335, 813-817.
3. J. D. Watson and F. H. Crick, *Nature*, 1953, 171, 737-738.
4. N. C. Seeman, *J Theor Biol*, 1982, 99, 237-247.
5. N. C. Seeman and N. R. Kallenbach, *Biophys J*, 1983, 44, 201-209.
6. J. H. Chen and N. C. Seeman, *Nature*, 1991, 350, 631-633.
7. D. Liu, S. H. Park, J. H. Reif and T. H. LaBean, *Proc Natl Acad Sci U S A*, 2004, 101, 717-722.
8. J. C. Mitchell, J. R. Harris, J. Malo, J. Bath and A. J. Turberfield, *J Am Chem Soc*, 2004, 126, 16342-16343.
9. P. W. Rothmund, A. Ekani-Nkodo, N. Papadakis, A. Kumar, D. K. Fygenon and E. Winfree, *J Am Chem Soc*, 2004, 126, 16344-16352.
10. H. Yan, S. H. Park, G. Finkelstein, J. H. Reif and T. H. LaBean, *Science*, 2003, 301, 1882-1884.
11. D. Liu, M. Wang, Z. Deng, R. Walulu and C. Mao, *J Am Chem Soc*, 2004, 126, 2324-2325.
12. P. W. K. Rothmund, *Nature*, 2006, 440, 297-302.
13. S. M. Douglas, H. Dietz, T. Liedl, B. Hogberg, F. Graf and W. M. Shih, *Nature*, 2009, 459, 1154-1154.
14. S. M. Douglas, J. J. Chou and W. M. Shih, *Proc Natl Acad Sci U S A*, 2007, 104, 6644-6648.
15. N. A. Bell, C. R. Engst, M. Ablay, G. Divitini, C. Ducati, T. Liedl and U. F. Keyser, *Nano Lett*, 2012, 12, 512-517.
16. M. Langecker, V. Arnaut, T. G. Martin, J. List, S. Renner, M. Mayer, H. Dietz and F. C. Simmel, *Science*, 2012, 338, 932-936.
17. R. Wei, T. G. Martin, U. Rant and H. Dietz, *Angew Chem Int Ed Engl*, 2012, 51, 4864-4867.
18. R. Jungmann, M. S. Avendano, J. B. Woehrstein, M. Dai, W. M. Shih and P. Yin, *Nat Methods*, 2014, 11, 313-318.
19. R. Jungmann, C. Steinhauer, M. Scheible, A. Kuzyk, P. Tinnefeld and F. C. Simmel, *Nano Lett*, 2010, 10, 4756-4761.

20. J. J. Schmied, C. Forthmann, E. Pibiri, B. Lalkens, P. Nickels, T. Liedl and P. Tinnefeld, *Nano Lett*, 2013, 13, 781-785.
21. H. T. Maune, S. P. Han, R. D. Barish, M. Bockrath, W. A. Iii, P. W. Rothmund and E. Winfree, *Nat Nanotechnol*, 2010, 5, 61-66.
22. H. Bui, C. Onodera, C. Kidwell, Y. Tan, E. Graugnard, W. Kuang, J. Lee, W. B. Knowlton, B. Yurke and W. L. Hughes, *Nano Lett*, 2010, 10, 3367-3372.
23. A. Kuzyk, R. Schreiber, Z. Y. Fan, G. Pardatscher, E. M. Roller, A. Hoge, F. C. Simmel, A. O. Govorov and T. Liedl, *Nature*, 2012, 483, 311-314.
24. R. Schreiber, J. Do, E. M. Roller, T. Zhang, V. J. Schuller, P. C. Nickels, J. Feldmann and T. Liedl, *Nat Nanotechnol*, 2014, 9, 74-78.
25. R. Schreiber, S. Kempter, S. Holler, V. Schuller, D. Schiffels, S. S. Simmel, P. C. Nickels and T. Liedl, *Small*, 2011, 7, 1795-1799.
26. Q. Jiang, C. Song, J. Nangreave, X. Liu, L. Lin, D. Qiu, Z. G. Wang, G. Zou, X. Liang, H. Yan and B. Ding, *J Am Chem Soc*, 2012, 134, 13396-13403.
27. Q. Zhang, Q. Jiang, N. Li, L. Dai, Q. Liu, L. Song, J. Wang, Y. Li, J. Tian, B. Ding and Y. Du, *ACS Nano*, 2014, 8, 6633-6643.
28. Y. X. Zhao, A. Shaw, X. Zeng, E. Benson, A. M. Nystrom and B. Hogberg, *ACS Nano*, 2012, 6, 8684-8691.
29. H. Lee, A. K. Lytton-Jean, Y. Chen, K. T. Love, A. I. Park, E. D. Karagiannis, A. Sehgal, W. Querbes, C. S. Zurenko, M. Jayaraman, C. G. Peng, K. Charisse, A. Borodovsky, M. Manoharan, J. S. Donahoe, J. Truelove, M. Nahrendorf, R. Langer and D. G. Anderson, *Nat Nanotechnol*, 2012, 7, 389-393.
30. N. V. Voigt, T. Topping, A. Rotaru, M. F. Jacobsen, J. B. Ravnsbaek, R. Subramani, W. Mamdough, J. Kjems, A. Mokhir, F. Besenbacher and K. V. Gothelf, *Nat Nanotechnol*, 2010, 5, 200-203.
31. A. Banerjee, D. Bhatia, A. Saminathan, S. Chakraborty, S. Kar and Y. Krishnan, *Angew Chem Int Ed Engl*, 2013, 52, 6854-6857.
32. S. M. Douglas, I. Bachelet and G. M. Church, *Science*, 2012, 335, 831-834.
33. M. Tintore, I. Gallego, B. Manning, R. Eritja and C. Fabrega, *Angew Chem Int Ed Engl*, 2013, 52, 7747-7750.
34. A. Udomprasert, M. N. Bongiovanni, R. Sha, W. B. Sherman, T. Wang, P. S. Arora, J. W. Canary, S. L. Gras and N. C. Seeman, *Nat Nanotechnol*, 2014, 9, 537-541.
35. B. Sacca, R. Meyer, M. Erkelenz, K. Kiko, A. Arndt, H. Schroeder, K. S. Rabe and C. M. Niemeyer, *Angew Chem Int Ed Engl*, 2010, 49, 9378-9383.
36. A. Shaw, V. Lundin, E. Petrova, F. Fordos, E. Benson, A. Al-Amin, A. Herland, A. Blokzijl, B. Hogberg and A. I. Teixeira, *Nat Methods*, 2014, 11, 841-846.
37. P. Wang, S. H. Ko, C. Tian, C. Hao and C. Mao, *Chem Commun (Camb)*, 2013, 49, 5462-5464.
38. A. Johnson-Buck, S. Jiang, H. Yan and N. G. Walter, *ACS Nano*, 2014, 8, 5641-5649.
39. N. D. Derr, B. S. Goodman, R. Jungmann, A. E. Leschziner, W. M. Shih and S. L. Reck-Peterson, *Science*, 2012, 338, 662-665.
40. C. Bustamante, S. B. Smith, J. Liphardt and D. Smith, *Curr Opin Struct Biol*, 2000, 10, 279-285.
41. J. Lipfert, J. W. Kerssemakers, T. Jager and N. H. Dekker, *Nat Methods*, 2010, 7, 977-980.
42. J. F. Marko and E. D. Siggia, *Macromolecules*, 1995, 28, 8759-8770.

43. M. D. Wang, H. Yin, R. Landick, J. Gelles and S. M. Block, *Biophys J*, 1997, 72, 1335-1346.
44. S. A. McKinney, A. C. Declais, D. M. Lilley and T. Ha, *Nature structural biology*, 2003, 10, 93-97.
45. M. A. Karymov, M. Chinnaraj, A. Bogdanov, A. R. Srinivasan, G. Zheng, W. K. Olson and Y. L. Lyubchenko, *Biophys J*, 2008, 95, 4372-4383.
46. D. J. Kauert, T. Kurth, T. Liedl and R. Seidel, *Nano Lett*, 2011, 11, 5558-5563.
47. D. N. Kim, F. Kilchherr, H. Dietz and M. Bathe, *Nucleic Acids Res*, 2012, 40, 2862-2868.
48. J. Yoo and A. Aksimentiev, *Proceedings of the National Academy of Sciences*, 2013, DOI: 10.1073/pnas.1316521110.
49. K. Pan, D. N. Kim, F. Zhang, M. R. Adendorff, H. Yan and M. Bathe, *Nat Commun*, 2014, 5, 5578.
50. P. Yin, R. F. Hariadi, S. Sahu, H. M. Choi, S. H. Park, T. H. Labean and J. H. Reif, *Science*, 2008, 321, 824-826.
51. D. Schiffels, T. Liedl and D. K. Fygenson, *ACS Nano*, 2013, 7, 6700-6710.
52. T. Liedl, B. Hogberg, J. Tytell, D. E. Ingber and W. M. Shih, *Nat Nanotechnol*, 2010, 5, 520-524.
53. H. Isambert, P. Venier, A. C. Maggs, A. Fattoum, R. Kassab, D. Pantaloni and M. F. Carlier, *J Biol Chem*, 1995, 270, 11437-11444.
54. M. M. Claessens, M. Bathe, E. Frey and A. R. Bausch, *Nat Mater*, 2006, 5, 748-753.
55. F. Gittes, B. Mickey, J. Nettleton and J. Howard, *J Cell Biol*, 1993, 120, 923-934.
56. F. Pampaloni, G. Lattanzi, A. Jonas, T. Surrey, E. Frey and E. L. Florin, *Proc Natl Acad Sci U S A*, 2006, 103, 10248-10253.
57. C. E. Castro, F. Kilchherr, D. N. Kim, E. L. Shiao, T. Wauer, P. Wortmann, M. Bathe and H. Dietz, *Nat Methods*, 2011, 8, 221-229.
58. C. Plesa, A. N. Ananth, V. Linko, C. Gulcher, A. J. Katan, H. Dietz and C. Dekker, *ACS Nano*, 2014, 8, 35-43.
59. E. Pfitzner, C. Wachauf, F. Kilchherr, B. Pelz, W. M. Shih, M. Rief and H. Dietz, *Angew Chem Int Ed Engl*, 2013, 52, 7766-7771.
60. L. Zhou, A. E. Marras, H. J. Su and C. E. Castro, *ACS Nano*, 2014, 8, 27-34.
61. C. Zhang, M. Su, Y. He, X. Zhao, P. A. Fang, A. E. Ribbe, W. Jiang and C. Mao, *Proc Natl Acad Sci U S A*, 2008, 105, 10665-10669.
62. H. Dietz, S. M. Douglas and W. M. Shih, *Science*, 2009, 325, 725-730.
63. D. Han, S. Pal, J. Nangreave, Z. Deng, Y. Liu and H. Yan, *Science*, 2011, 332, 342-346.
64. D. Han, S. Pal, Y. Yang, S. Jiang, J. Nangreave, Y. Liu and H. Yan, *Science*, 2013, 339, 1412-1415.
65. M. J. Lang, P. M. Fordyce, A. M. Engh, K. C. Neuman and S. M. Block, *Nat Methods*, 2004, 1, 133-139.
66. M. Eriksson and P. E. Nielsen, *Quarterly reviews of biophysics*, 1996, 29, 369-394.
67. A. Rajendran, M. Endo, Y. Katsuda, K. Hidaka and H. Sugiyama, *J Am Chem Soc*, 2011, 133, 14488-14491.
68. K. Svoboda and S. M. Block, *Cell*, 1994, 77, 773-784.
69. J. H. Shin, B. K. Tam, R. R. Brau, M. J. Lang, L. Mahadevan and P. Matsudaira, *Biophys J*, 2007, 92, 3729-3733.
70. D. R. Han, S. Pal, Y. Liu and H. Yan, *Nat Nanotechnol*, 2010, 5, 712-717.

71. B. Yurke, A. J. Turberfield, A. P. Mills, Jr., F. C. Simmel and J. L. Neumann, *Nature*, 2000, 406, 605-608.
72. H. Gu, W. Yang and N. C. Seeman, *J Am Chem Soc*, 2010, 132, 4352-4357.
73. A. Kuzuya, Y. Sakai, T. Yamazaki, Y. Xu and M. Komiyama, *Nat Commun*, 2011, 2, 449.
74. E. S. Andersen, M. Dong, M. M. Nielsen, K. Jahn, R. Subramani, W. Mamdouh, M. M. Golas, B. Sander, H. Stark, C. L. Oliveira, J. S. Pedersen, V. Birkedal, F. Besenbacher, K. V. Gothelf and J. Kjems, *Nature*, 2009, 459, 73-76.
75. R. M. Zadegan, M. D. Jepsen, K. E. Thomsen, A. H. Okholm, D. H. Schaffert, E. S. Andersen, V. Birkedal and J. Kjems, *ACS Nano*, 2012, 6, 10050-10053.
76. C. Mao, W. Sun, Z. Shen and N. C. Seeman, *Nature*, 1999, 397, 144-146.
77. D. Y. Zhang and G. Seelig, *Nat Chem*, 2011, 3, 103-113.
78. N. Srinivas, T. E. Ouldridge, P. Sulc, J. M. Schaeffer, B. Yurke, A. A. Louis, J. P. Doye and E. Winfree, *Nucleic Acids Res*, 2013, 41, 10641-10658.
79. H. Yan, X. Zhang, Z. Shen and N. C. Seeman, *Nature*, 2002, 415, 62-65.
80. D. Y. Zhang, A. J. Turberfield, B. Yurke and E. Winfree, *Science*, 2007, 318, 1121-1125.
81. T. Omabegho, R. Sha and N. C. Seeman, *Science*, 2009, 324, 67-71.
82. P. Yin, H. Yan, X. G. Daniell, A. J. Turberfield and J. H. Reif, *Angew Chem Int Ed Engl*, 2004, 43, 4906-4911.
83. B. Ding and N. C. Seeman, *Science*, 2006, 314, 1583-1585.
84. K. Lund, A. J. Manzo, N. Dabby, N. Michelotti, A. Johnson-Buck, J. Nangreave, S. Taylor, R. Pei, M. N. Stojanovic, N. G. Walter, E. Winfree and H. Yan, *Nature*, 2010, 465, 206-210.
85. T. G. Cha, J. Pan, H. Chen, J. Salgado, X. Li, C. Mao and J. H. Choi, *Nat Nanotechnol*, 2014, 9, 39-43.
86. H. Gu, J. Chao, S. J. Xiao and N. C. Seeman, *Nature*, 2010, 465, 202-205.
87. L. Qian and E. Winfree, *Science*, 2011, 332, 1196-1201.
88. L. Qian, E. Winfree and J. Bruck, *Nature*, 2011, 475, 368-372.
89. D. Y. Zhang, R. F. Hariadi, H. M. Choi and E. Winfree, *Nat Commun*, 2013, 4, 1965.
90. F. Zhang, J. Nangreave, Y. Liu and H. Yan, *Nano Lett*, 2012, 12, 3290-3295.
91. A. Kuzyk, R. Schreiber, H. Zhang, A. O. Govorov, T. Liedl and N. Liu, *Nat Mater*, 2014, 13, 862-866.
92. L. Feng, S. H. Park, J. H. Reif and H. Yan, *Angew Chem Int Ed Engl*, 2003, 42, 4342-4346.
93. A. E. Marras, L. Zhou, H. J. Su and C. E. Castro, *Proc Natl Acad Sci U S A*, 2015, DOI: 10.1073/pnas.1408869112.
94. G. J. Lavella, A. D. Jadhav and M. M. Maharbiz, *Nano Lett*, 2012, 12, 4983-4987.
95. J. Fu, Y. R. Yang, A. Johnson-Buck, M. Liu, Y. Liu, N. G. Walter, N. W. Woodbury and H. Yan, *Nat Nanotechnol*, 2014, 9, 531-536.
96. A. N. Marchi, I. Saaem, B. N. Vogen, S. Brown and T. H. LaBean, *Nano Lett*, 2014, 14, 5740-5747.